

DISCLAIMER

This report was prepared as an account of work sponsored by the U.S. Government. Neither the United States nor any agency thereof, nor any of their employees, makes any warranty, express or implied, or assumes any legal liability or responsibility for the accuracy, completeness, or usefulness of any information, apparatus, product, or process disclosed, or represents that its use would not infringe privately owned rights. Reference herein to any specific commercial product, process, or service by trade name, trademark, manufacturer, or otherwise, does not necessarily constitute or imply its endorsement, recommendation, or favoring by the U.S. Government or any agency thereof. The views and opinions of authors expressed herein do not necessarily state or reflect those of the U.S. Government or any agency thereof.

GVR Radiometer Handbook

MP Cadeddu

March 2011

Work supported by the U.S. Department of Energy,
Office of Science, Office of Biological and Environmental Research

Contents

1.0	General Overview.....	1
2.0	Contacts.....	1
2.1	Mentor.....	1
2.2	Vendor / Instrument Developer.....	1
3.0	Deployment Locations and History.....	1
4.0	Near-Real-Time Data Plots.....	2
5.0	Data Description and Examples.....	2
5.1	Data File Contents.....	2
5.1.1	Primary Variables and Expected Uncertainty.....	2
5.1.2	Secondary / Underlying Variables.....	3
5.1.3	Diagnostic Variables.....	3
5.1.4	Data Quality Flags.....	3
5.1.5	Dimension Variables.....	4
5.2	Annotated Examples.....	4
5.3	User Notes and Known Problems.....	4
5.4	Frequently Asked Questions.....	5
6.0	Data Quality.....	5
6.1	Data Quality Health and Status.....	5
6.2	Data Reviews by Instrument Mentor.....	5
6.3	Data Assessments by Site Scientist / Data Quality Office.....	5
6.4	Value-Added Procedures and Quality Measurement Experiments.....	5
7.0	Instrument Details.....	6
7.1	Detailed Description.....	6
7.1.1	List of Components.....	6
7.1.2	System Configuration and Measurement Methods.....	6
7.1.3	Specifications.....	7
7.2	Theory of Operation.....	7
7.3	Calibration.....	8
7.3.1	Theory.....	8
7.3.2	Procedures.....	9
7.3.3	History.....	10
7.4	Operation and Maintenance.....	10
7.4.1	User Manual.....	10
7.4.2	Routine and Corrective Maintenance Documentation.....	10
7.4.3	Software Documentation.....	10
7.4.4	Additional Documentation.....	10
7.5	Glossary.....	10
7.6	Acronyms.....	10
7.7	Citable References.....	11

Figures

1	GVR simplified component level block diagram.	6
2	GVR-measured brightness temperatures as a function of PWV retrieved from the collocated MWR	8

Tables

1	Status and Location of the GVR.	1
2	Primary Variables.	2
3	Secondary Variables.	3
4	Diagnostic Variables.	3
5	Data Quality Thresholds.	4
6	Dimension Variables.	4
7	Instrument specifications.	7

1.0 General Overview

The G-Band Vapor Radiometer (GVR) provides time-series measurements of brightness temperatures from four double sideband channels centered at ± 1 , ± 3 , ± 7 , and ± 14 GHz around the 183.31-GHz water vapor line. Atmospheric emission in this spectral region is primarily due to water vapor, with some influence from liquid water. The 183.31 ± 14 -GHz channel is particularly sensitive to the presence of liquid water. The sensitivity to water vapor of the 183.31-GHz line is approximately 30 times higher than at the frequencies of the two-channel microwave radiometer (MWR) for a precipitable water vapor (PWV) amount of less than 2.5 mm. Measurements from this instrument are therefore especially useful during low-humidity conditions (PWV < 5 mm).

2.0 Contacts

2.1 Mentor

Maria Cadeddu
 Computing Environment and Life Sciences
 Argonne National Laboratory, Bldg. 240
 Argonne, Illinois 60439
 630.252.7408
mcadeddu@anl.gov

2.2 Vendor / Instrument Developer

ProSensing, Inc.
 107 Sunderland Road
 Amherst, Massachusetts 01002
 413.549.4402
info@prosensing.com

3.0 Deployment Locations and History

Table 1. Status and Location of the GVR.

Serial Number	Property Number	Location	Date Installed	Date Removed	Status
001		NSA/C1	2000/09/1		Operational

4.0 Near-Real-Time Data Plots

Plots of near-real-time data can be viewed at the DQHands (Data Quality Health and Status) system accessible through the web page: <http://dq.arm.gov/>. Click on “QC Metrics and Plots” and select the desired site and datastream. The GVR is located at the site “North Slope of Alaska” (NSA), the datastream is “nsagvrC1.b1” or “nsagvrC1.a0” and the facility is “C1.” A value-added product datastream “nsagvrC1.c1” provides retrievals of Precipitable Water Vapor.

5.0 Data Description and Examples

5.1 Data File Contents

Datastreams available from the ARM Data Archive are:

- **nsagvrC1.a0:** Raw signal counts at all frequencies
- **nsagvrC1.b1:** Calibrated, unfiltered and filtered brightness temperatures
- **nsagvrC1.c1:** Calibrated brightness temperatures and precipitable water vapor retrievals

5.1.1 Primary Variables and Expected Uncertainty

The primary variables measured by the GVR are brightness temperatures at 183.31 ± 1 , 183.31 ± 3 , 183.31 ± 7 , and 183.31 ± 14 -GHz. Because of some interference caused by a nearby U.S. Air Force radar, a filter is routinely applied to all data. In the nsagvrC1.b1 datastream, there are two sets of brightness temperatures: one is the original time-series with interference spikes, and the second one is the filtered time series.

Table 2. Primary Variables.

Variable Name	Quantity Measured	Unit	Uncertainty
tbsky1	183.3 ± 1 GHz sky brightness temperature (filtered)	K	2 K
tbsky3	183.3 ± 3 GHz sky brightness temperature (filtered)	K	2 K
tbsky7	183.3 ± 7 GHz sky brightness temperature (filtered)	K	2 K
tbsky14	183.3 ± 14 GHz sky brightness temperature (unfiltered)	K	2 K
tbsky1u	183.3 ± 1 GHz sky brightness temperature (unfiltered)	K	2 K
tbsky3u	183.3 ± 3 GHz sky brightness temperature (unfiltered)	K	2 K
tbsky7u	183.3 ± 7 GHz sky brightness temperature (unfiltered)	K	2 K
tbsky14u	183.3 ± 14 GHz sky brightness temperature (filtered)	K	2 K

5.1.2 Secondary / Underlying Variables

Table 3. Secondary Variables.

Variable Name	Quantity Measured	Unit	Uncertainty
time	Time offset from midnight	s	
temp_ext	Temperature at the surface	K	2.0
warm1	183.3 ± 1 GHz warm load signal	count	
warm3	183.3 ± 3 GHz warm load signal	count	
warm7	183.3 ± 7 GHz warm load signal	count	
warm14	183.3 ± 14 GHz warm load signal	count	
hot1	183.3 ± 1 GHz hot load signal	count	
hot3	183.3 ± 3 GHz hot load signal	count	
hot7	183.3 ± 7 GHz hot load signal	count	
hot14	183.3 ± 14 GHz hot load signal	count	
sky1	183.3 ± 1 GHz sky signal	count	
sky3	183.3 ± 3 GHz sky signal	count	
sky7	183.3 ± 7 GHz sky signal	count	
sky14	183.3 ± 14 GHz sky signal	count	

5.1.3 Diagnostic Variables

Table 4. Diagnostic Variables.

Variable Name	Quantity Measured	Unit	Uncertainty
temp_hot1	Temperature of the hot absorber at the tip	C	0.2 K
temp_hot2	Temperature of the hot absorber at the center	C	0.2 K
temp_warm	Temperature of the warm absorber	C	0.2 K
temp_component_plate	Physical temperature of component plate	C	
temp_antenna_feed_horn	Physical temperature of antenna feed horn	C	
temp_thermoelectric_cooling_plate	Physical temperature of thermoelectric cooling plate	C	

5.1.4 Data Quality Flags

Data quality flags are named qc_‘fieldname’ (i.e. qc_tbsky1). Possible values for qc_flags are: 0 (value is within the specified range), 1 (missing value), 2 (value is less than the specified minimum), 4 (value is greater than the specified maximum), and 8 (value failed the valid “delta” check). Specified maximum and minimum values are shown in Table 5.

Table 5. Data Quality Thresholds.

Field Name	Min	Max
tbsky1	3	310
tbsky3	3	310
tbsky7	3	310
tbsky14	3	310
temp_hot1	45	75
temp_hot2	45	75
temp_warm	10	20

5.1.5 Dimension Variables

Table 6. Dimension Variables.

Field Name	Quantity	Unit
base_time	Base time in Epoch	seconds since 1970-1-1 0:00:00 0:00
time_offset	Time offset from base_time	s
lat	north latitude	degrees
lon	east longitude	degrees
alt	altitude	meters above Mean Sea Level

Some additional variables defined in the global fields are:

- delta_time_warm = time difference between the observation of the sky and the warm target = 4 s
- delta_time_hot = time difference between the observation of the sky and the hot target=2 s

5.2 Annotated Examples

This section not yet available.

5.3 User Notes and Known Problems

Users should use only filtered data (tbsky1, tbsky3, tbsky7, and tbsky14). Unfiltered data (tbsky1u, tbsky3u, tbsky7u, and tbsky14u) have high noise levels and should be avoided.

Between 4/12/2004 and 9/1/2006 the instrument was working as a prototype. Data collected during this time have segments of elevated noise due to a slowly varying reduction of receiver sensitivity. This effect was dependent on the system temperature, and it is noticeable during warmer days (surface temperatures $> \sim 255$ K).

5.4 Frequently Asked Questions

This section is not available.

6.0 Data Quality

6.1 Data Quality Health and Status

Daily quality check on this datastream can be found at the DQHands page: <http://dq.arm.gov/>. Click on “QC Metrics and Plots” and select the desired site and datastream. The GVR is located at the site “NSA”, the datastream is “nsagvrC1.b1” or “nsagvrC1.a0” and the facility is “C1”.

6.2 Data Reviews by Instrument Mentor

The instrument mentor submits a monthly summary report IMMS accessible from the instrument web page. Some of the general checks performed by the instrument mentor are shown below.

1. In general the filtered brightness temperature time series should be smooth and with low noise levels.
2. Brightness temperatures should be greater than 2.75 K and less than approximately 310 K (We do not expect the ambient temperature in Barrow to be significantly higher than 30°C).
3. External temperature readings (ext_temp) can be compared to tower measurements. The agreement should be +/- 2 K.
4. The difference between the tip and the center of the hot absorbet (t_hot1-t_hot2) should be less than 2°C.
5. The temperature of the hot target (temp_hot1 and T_hot2) should be greater than 45°C and less than 75°C.
6. The temperature of the warm target should be greater than 10°C and less than 20°C.
7. Measured brightness temperatures are also compared with model computations as a general quality check.

6.3 Data Assessments by Site Scientist / Data Quality Office

The Data Quality office daily data assessment can be viewed at the [DQHands](#) web page.

6.4 Value-Added Procedures and Quality Measurement Experiments

Water vapor retrievals are available as a value-added product for this instrument. The retrievals are in the datastream nsagvrC1.c1. The variable name is “pwv” and the associated uncertainty is “pw_error”. Details of the algorithm can be found in [1].

7.0 Instrument Details

7.1 Detailed Description

7.1.1 List of Components

- RF section: white plastic box with rectangular Mylar window on top
- Desktop PC host computer with monitor, keyboard, and mouse, and National Instrument break-out box mounted on top of PC enclosure.
- Temperature control box
- Radiometer cart with industrial blower on bottom shelf
- Cables

7.1.2 System Configuration and Measurement Methods

In this section we give a brief description of the GVR hardware configuration. The material in this section can be found in [2]. Refer to the same reference for further details on this instrument. A simplified block diagram of the GVR receiver is shown in Figure 2. The downwelling atmospheric radiation is captured by a 10-cm diameter, 1.7° beamwidth, 90-degree parabolic metal mirror and focused to a corrugated feed horn. A sub-harmonically pumped mixer, using a 91.655-GHz LO signal, down-converts the upper and lower sidebands to base-band, where a broadband low-noise amplifier increases the noise signal power and sets the receiver noise temperature. A broadband power splitter divides the amplified signal between four channels before filtering. The center frequency and bandwidth of the filters are 1/0.5, 3/1, 7/1.4, and 14/2 GHz respectively. The band-limited noise signals are square-law detected, converted to a TTL pulse-train using highly linear Analog Devices AD650 voltage-to-frequency converters (20 ppm nonlinearity and less than 0.3 ms response time to a step input as configured), and frequency-counted using an FPGA processor. This frequency counting effectively integrates and measures the square-law detector voltage, or equivalently the noise power. The measured noise power from the four channels together with the instrument temperature readings are time-stamped and transmitted to a data logger PC via an RS232 (or optional RS422) bus.

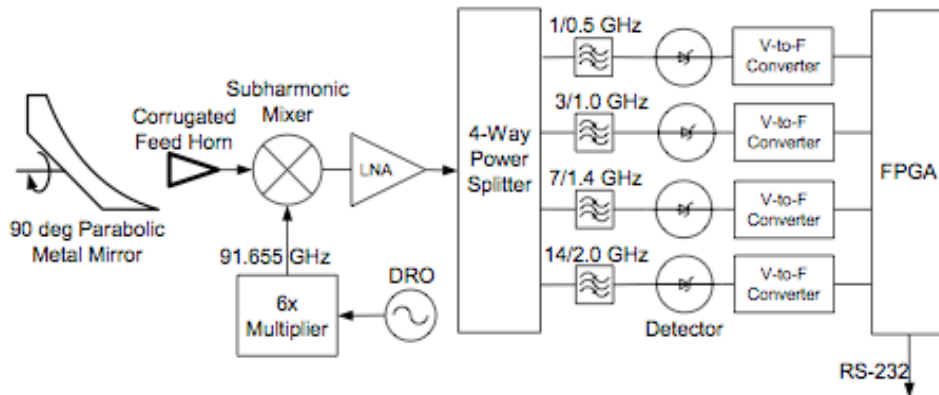


Figure 1. GVR simplified component level block diagram.

To stabilize the temperature of the receiver components, a packaging technique was employed, consisting of an insulated cold plate in a box, in a temperature-controlled enclosure. The resulting component plate temperature stability limited the effect of receiver-gain rate-of-change to below 100 K/Hr, requiring system gain and offset calibrations only a few times a minute to achieve a sub-K measurement precision.

Since neither noise sources nor low-loss fast switches are readily available at G-band, external (to the antenna horn) hot and warm calibration absorbers are required to track the receiver gain and offset. The metal mirror of the GVR is rotated with a stepper motor to point the radiometer antenna beam to the calibration loads. The hot and warm calibration absorbers are constructed using the Firam-160 absorber, with the hot load packed in an insulated box covered with a 1-mil Mylar window (~ 0.03 dB loss factor) tilted by 4° . The Mylar window is tilted by about twice the antenna beamwidth to minimize the reflection of the receiver-emitted radiation back to the receiver. The hot load is convection-heated to a uniform temperature of 343 ± 0.5 K, while the warm load is left to soak to the temperature of the outer enclosure, which is heated with a PID controller to 293 K. The temperature of the absorbers is monitored with Resistance Temperature Detectors (RTD) temperature sensors, and the readings are recorded along with the receiver noise power data.

7.1.3 Specifications

Table 7. Instrument specifications.

Parameter	Value
Receiver noise temperature 1 GHz	1750 K
Receiver noise temperature 3 GHz	1610 K
Receiver noise temperature 7 GHz	1600 K
Receiver noise temperature 14 GHz	2170 K
Measurement precision, NEDT (Noise Equivalent Delta-T)	0.2 K
Measurement Stability (Allan STD)	< 0.05 K over 1000 s
Measurement rate	10/min with continuous calibration
Antenna aperture	4"
Antenna beamwidth	1.5°
Temperature range	-40 to 10 C
Output	ASCII data files

7.2 Theory of Operation

The GVR measures brightness temperatures from four double-sideband channels centered at ± 1 , ± 3 , ± 7 , and ± 14 GHz around the 183.31-GHz water-vapor line. Atmospheric emission in this spectral region is primarily due to water vapor, with some influence from liquid water. The 183.31 ± 3 and 183.31 ± 14 -GHz channels are particularly sensitive to the presence of liquid water.

The sensitivity of the GVR channels to the presence of water vapor is much stronger than that of the 22-GHz water vapor line. In Figure 2 the dependence of GVR-measured clear-sky brightness temperatures on PWV is shown [3]. The PWV is retrieved from the MWR measurements. The circles,

diamonds, triangles, and squares are model computations from one year of radiosonde data. Figure 2 shows the nonlinear response of the GVR to water vapor as well as the saturation of the channels close to the line center. These results are consistent with those of [3], who estimated the sensitivity to PWV at these frequencies to be approximately 30 times higher than at the frequencies of the MWR for PWV less than 2.5 mm. The 183.31 ± 14 GHz channel sensitivity to liquid water path is about 3.5 times greater than the sensitivity of the 31.4-GHz channel of the MWR [3].

The sensitivity of this channel to ice scattering is negligible (< 0.6 K) at the GVR frequencies for typical winter ice clouds. Since the presence of ice water path will increase the brightness temperature observed by the 183.3 ± 14 GHz channel, the presence of ice water path would be interpreted as a contribution from liquid clouds.

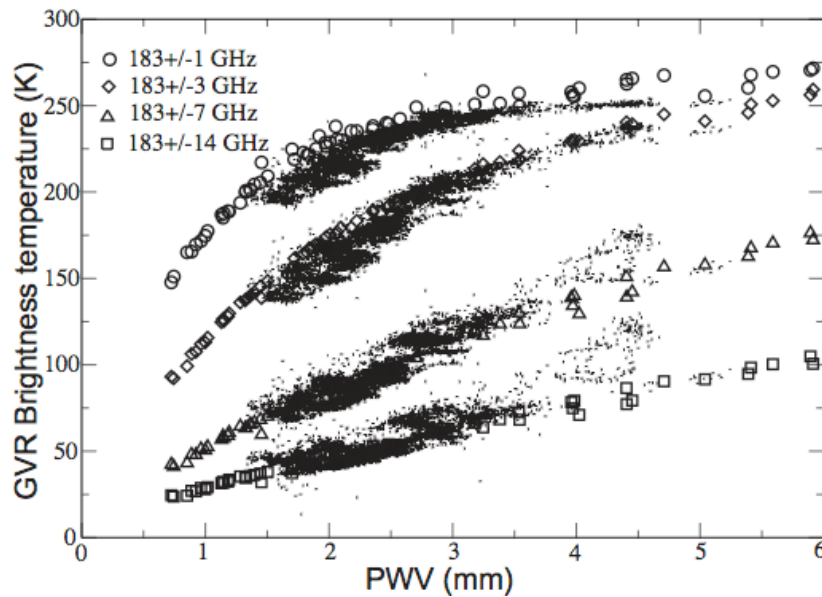


Figure 2. GVR-measured brightness temperatures as a function of PWV retrieved from the collocated MWR. Data are for non-cloudy conditions only. The circles, diamonds, triangles, and squares are model computations from one year of radiosonde data. The nonlinear response to PWV is evident in the ± 1 and ± 3 channels [3].

7.3 Calibration

7.3.1 Theory

The GVR is calibrated using a warm (~ 293 K) and a hot (~ 333 K) FIRAM-160 absorber. The absorbers are tilted by about 10 degrees to ensure better than -60 dB reflectivity or 0.999999 emissivity. The resulting absorber brightness temperatures are taken to be equal to their physical temperature. The warm load “floats” at the internal temperature of the GVR enclosure. The hot load, packaged in an insulated box with a Mylar window, is convection-heated; behind the absorber (opposite of the Mylar window) is a heated metal plate and a row of fans. The fans circulate the air around the load indirectly heating it. RTD placed at several locations in and around the hot load indicate that the maximum temperature differences are less than 0.5 K. The average temperature reported by sensors is used as the hot load equivalent

brightness temperature. The accuracy of the temperature sensors is approximately 0.2 K, making them the most significant source of calibration error. This is because a + 0.2 K error at the 333 K hot load temperature and a -0.2 K error at the 293 K warm load temperature will amplify to a -2.8 K error at a 33 K sky brightness temperature. The metal mirror of the radiometer continuously cycles between the warm load, hot load, and the sky, calibrating the instrument once every 10 seconds. This calibration is sufficiently frequent as the Allan Deviation stability of the GVR receiver was measured to be less than 0.05 K at a ΔT of 1000 sec. The operational calibration of the GVR was independently verified in the spring of 2006 with an external calibration load. A larger insulated hot-load convection chamber was constructed with a higher precision temperature meter and sensors, calibrated with a NIST-traceable voltmeter and temperature probe with a 0.05 K absolute accuracy. The measured absolute error was less than 2 K in the four receiver channels over the brightness temperature measurement range. The brightness temperatures used in this paper are the ones originally obtained from the instrument. The revised calibration produced a slight (~ 1 K) increase in the brightness temperatures of the ± 1 and ± 3 -GHz channel, slightly improving the agreement with the model. In the next section we will apply the calibration correction to a few cases to determine the possible contribution of calibration uncertainties to the measurement.

7.3.2 Procedures

Brightness temperatures T'_{sky} are produced for each channel according to:

$$T'_{sky} = T_{warm} + G(V_{sky} - V_{warm}), \quad (1)$$

Where V_{sky} is the signal recorded when the reflector is oriented towards the sky, and V_{warm} is the signal recorded from the warm target at temperature T . G is the gain computed as:

$$G = \frac{\bar{T}_{hot} - T_{warm}}{V_{hot} + V_{warm}}, \quad (2)$$

where V_{hot} is the signal recorded from the hot target, and \bar{T}_{hot} is computed by averaging the temperature of the hot target at the tip (T_{hot1}) and at the center (T_{hot2}):

$$\bar{T}_{hot} = 0.5(T_{hot1} + T_{hot2}), \quad (3)$$

Keeping into account the Mylar loss factor $L = 1.0116$, the final brightness temperature is computed as:

$$T_{sky} = L(T'_{sky} + 273) + (1 - L)293 \quad (4)$$

A filter is applied to the raw data (counts) as well as to the final brightness temperatures to produce the final brightness temperatures. The filter acts to ensure that each data point is bounded within the range of intensities defined by its neighbors. For each data point, the maximum and minimum values of the first four neighbors are determined. If the difference between the point and the maximum (or the minimum) is greater than a fixed threshold (in this case set to 3 K), the point is replaced with the average of the four neighbors. This filter is less smoothing than a traditional median filter as it trades noise suppression for temporal resolution.

7.3.3 History

- Deployed as SBIR prototype in Barrow, Alaska on April 14, 2005
- Calibration verified with external calibration box on April 19, 2006
- Factory hardware upgrades on May–August 2006
- Reinstallation in Barrow on September 1, 2006

7.4 Operation and Maintenance

7.4.1 User Manual

Contact the Instrument Mentor.

7.4.2 Routine and Corrective Maintenance Documentation

Not available.

7.4.3 Software Documentation

Not available.

7.4.4 Additional Documentation

This section is not applicable to this document.

7.5 Glossary

Uncertainty: We define uncertainty as the range of probable maximum deviation of a measured value from the true value within a 95% confidence interval. Given a bias (mean) error B and uncorrelated random errors characterized by a variance s^2 , the root-mean-square error (RMSE) is defined as the vector sum of these,

$$RMSE = (B^2 + \sigma^2)^{1/2} \quad (5)$$

(B may be generalized to be the sum of the various contributors to the bias and s^2 the sum of the variances of the contributors to the random errors). To determine the 95% confidence interval we use the Student's t distribution: $t_{n,0.025} \approx 2$, assuming the RMSE was computed for a reasonably large ensemble. Then the *uncertainty* is calculated as twice the RMSE.

7.6 Acronyms

See the list of [acronyms](#) on the ARM website.

7.7 Citable References

Cadeddu, MP, DD Turner, and JC Liljegren. 2009. "A Neural Network for Real-Time Retrievals of PWV and LWP From Arctic Millimeter-Wave Ground-Based Observations." *IEEE Transactions on Geoscience and Remote Sensing* 47(7): 1887–1900.

Pazmany, AL. 2007. "A compact 183 GHz radiometer for water vapor and liquid sensing." *IEEE Transactions on Geoscience and Remote Sensing* 45(7): 2202–2207.

Cadeddu, MP, JC Liljegren, and AL Pazmany. 2007. "Measurements and retrievals from a new 183-GHz water-vapor radiometer in the arctic." *IEEE Transactions on Geoscience and Remote Sensing* 45(7): 2207–2215.



U.S. DEPARTMENT OF
ENERGY

Office of Science